Time-Frequency Analysis of Nonstationary Wind Speed using Stationary Wavelet Transform and Empirical Mode Decomposition

*Ming-Jie Zhang[1], Fu-You Xu[2] and Xiu-Yong Wang[3]

[1], [2] *School of Civil Engineering, Dalian University of Technology, Dalian, China*
[3] *School of Civil Engineering, Hunan University of Science and Technology, Xiangtan China*
[1] *mingjiezhg@hotmail.com*

ABSTRACT

The extreme wind speeds induced by typhoon Rammasun are analyzed, both the longitudinal and lateral wind speeds show clearly nonstationary features. The nonstationary wind speeds can be modeled as the summations of time-varying mean components and fluctuating components. The stationary wavelet transform and empirical mode decomposition are used to extract the time-varying means. Results show that the time-varying means extracted by these two methods are quite consistent. The Hilbert energy spectra are used to characterize the time-frequency distributions of the nonstationary wind speeds. It is found that the energies of the fluctuating components are mostly distributed in the region with frequency lower than 0.1 Hz. The frequency modulations of the fluctuating components are weak, indicating that the fluctuating components can be modeled as uniformly modulated nonstationary processes.

1. INTRODUCTION

The stationary boundary-layer winds have been traditionally dealt with by the stationary model proposed by Davenport (1961, 1967). However, extreme winds induced by typhoons, thunderstorm downbursts, and tornadoes show clearly nonstationary features, making the stationary model difficult to characterize these events. Compared with the stationary processes, the frequency contents and amplitudes for nonstationary processes may be time-varying. The traditional Fourier transform just gives a time averaged spectral distribution, and cannot reveal the transient features of a nonstationary process. To describe the time-varying characteristics of nonstationary processes, advanced time-frequency analysis tools have been developed, including the

---

[1] Ph.D. Candidate
[2] Associate Professor
[3] Professor

short-time Fourier transform (STFT), the Wigner-Ville distribution (WVD), the wavelet transform (WT) and the empirical mode decomposition (EMD) with Hilbert transform.

The STFT uses a constant width window to capture the time-frequency distribution, and therefore the time-frequency resolutions are limited. The WVD always yield ghost terms as the consequence of the bilinearity of the transform (Carmona et al. 1998). A more widely used representation can be achieved by the WT, which project a signal onto a set of basis functions which are simply dilations and/or translations of a parent wavelet with localized energies in both time and frequency domains. The window size of WT can be adjusted, i. e., narrower for high frequency and wider for low frequency contents, which lead to high resolutions for the whole region. Kareem and Kijewski (2002) overviewed some developments in the wavelet-based time-frequency analysis in the civil engineering domain. Spanos and Failla (2004) estimated the evolutionary power spectra density through a wavelet-based method. Olhede and Walden (2004) combined the stationary WT with the Hilbert spectrum to characterize the time–frequency distributions of nonstationary signals. The same method was also applied by Wang et al. (2013a; 2013b).

On the other hand, Huang et al. (1998) proposed the EMD to adaptively decompose the complicated signals into a finite number of nearly narrow band signals termed as intrinsic mode functions (IMFs) and a final residue. After the decomposition, Hilbert transform can be applied to get the instantaneous characteristics of each IMF. The Hilbert spectrum of the signal can then be generated, which is a representation of the time-frequency distribution of the signal. Zhang et al. (2003) analyzed the time-frequency features of ground motions through EMD with Hilbert transform and concluded that the method captures the time-frequency distribution accurately. Li and Wu (2007) used the EMD with Hilbert transform to analyze the nonstationary characteristics of wind speeds and typhoon-induced responses of a tall building. More recently, a new noise-assistant method, i. e., the ensemble EMD (EEMD) was developed (Wu and Huang 2009) to deal with the problem of mode mixing in EMD. The superiorities of EEMD relative to EMD in decomposing complicated signals were proved by Wu and Huang (2009).

In this study, the theoretical backgrounds concerning the SWT, EEMD, and normalized Hilbert transform (NHT) are briefly presented. The SWT and EEMD are then used to decompose the nonstationary wind speed data into time-varying means and fluctuating components. Results show that the mean components extracted by SWT and EEMD are quite consistent. The NHT method is used to calculate the instantaneous amplitudes and frequencies of the fluctuating components, and the Hilbert energy spectra are used to characterize the time-frequency distributions. It is found that the energies of the fluctuating components are mostly distributed in the frequency band lower than 0.1 Hz. The frequency modulations of the fluctuating components are weak, indicating that the fluctuating components can be modeled as uniformly modulated nonstationary processes.

2. Theoretical Backgrounds

2.1 *Stationary Wavelet Transform*

As the SWT is a special version of the discrete WT (DWT), a brief introduction of the DWT is necessary for understanding the SWT. The DWT projects a signal $x(t)$ onto a set of wavelet basis functions, which are the dilations or translations of a parent wavelet $\psi(t)$ (Mallet 1989)

$$W_\psi(2^j, b) = \left\langle x(t), \psi(\frac{t-b}{2^j}) \right\rangle, (1)$$

where j is the decomposition level; 2^j is the discrete dilation factor; b is the translation factor; $\psi(\frac{t-b}{2^j})$ is the wavelet function after dilation of 2^j and transition of b. $W_\psi(a, b)$ is the wavelet coefficient corresponding to $\psi(\frac{t-b}{2^j})$

The DWT behaves as a dyadic filter bank and leads to a multi-resolution decomposition of the signal, i. e.,

$$x(t) = \sum_{i=1}^{m} D_i(t) + A_m(t), (2)$$

where $D_i(t)$ (i = 1 to m) is the detail function of the ith decomposition level; $A_m(t)$ is the approximation function. The frequency band of the ith detail function is $f_s/2^{i+1}$ to $f_s/2^i$ Hz, and the frequency band of the approximation component is 0 to $f_s/2^{m+1}$ Hz, where f_s is the sampling frequency of $x(t)$.

In the standard DWT, a decimation (down-sampling) operation is conducted at each decomposition level, and therefore leads to the problem of shift variance (Mallat 1989). The SWT abandons the decimation operation, and applies appropriate filters at each level to produce two sequences for the next level (Holschneider et al., 1989; Percival and Walden, 2000). The SWT provides a redundant representation of the signal, making it exhibit the property of shift-invariance and perform better in restruction (Daubechies, I. 2004).

2.2 *Ensemble Empirical Mode Decomposition*
The empirical mode decomposition (EMD) was firstly proposed by Huang et al. (1998) to adaptively decompose a complicated signal $x(t)$ into a finite number of amplitude-frequency modulated intrinsic mode functions (IMFs) and a final residue, i.e.,

$$x(t) = \sum_{i=1}^{m} c_i(t) + r(t), (3)$$

where $c_i(t)$ (i = 1 to m) are the IMFs; $r(t)$ is the final residue.

Recently, the ensemble EMD (EEMD) (Wu and Huang 2009) is developed to deal with the problem of mode mixing in EMD. EEMD involves of a noise-assistant method in which the interactive shifting process is applied on a number of white noise-added

signals, and the mean is treated as the final result. Detailed introductions on the EMD and EEMD can be found in Huang et al. (1998) and Wu and Huang (2009).

2.3 *Instantaneous Amplitude and Instantaneous Frequency*

For a monocomponent signal $y(t)$ with amplitude and frequency modulation

$$y(t) = a(t)\cos[\varphi(t)], (4)$$

where $a(t)$ is the instantaneous amplitude; $\varphi(t)$ is the instantaneous phase. The analytic signal $z(t)$ of $y(t)$ is obtained as

$$z(t) = y(t) + iH[y(t)], (5)$$

where $i = \sqrt{-1}$; $H[y(t)]$ is the Hilbert transform of $y(t)$. The instantaneous amplitude and frequency can be respectively calculated as

$$a(t) = \sqrt{y^2(t) + H^2[y(t)]}, (6)$$

$$f(t) = \frac{1}{2\pi} d\varphi(t) \Big/ dt = \frac{1}{2\pi} d(\arctan \frac{H(y(t))}{y(t)}) \Big/ dt, (7)$$

However, direct application of Eq. (7) may produce large frequency modulation, and even results in negative frequencies at some time instants. Huang et al. (2009) proposed the normalized Hilbert transform (NHT), in which $y(t)$ is normalized by its cubic spline fitted envelope, i.e.,

$$y_1(t) = \frac{y(t)}{e_1(t)}, (8)$$

where $y_1(t)$ is the normalized signal; $e_1(t)$ is the cubic spline fitted envelope of $y(t)$. As $e_1(t)$ is generally different from the instantaneous amplitude of $y(t)$, the normalization needs to be implemented repeatedly to ensure all values of the normalized signal are less than or equal to unity, i. e.,

$$y_2(t) = \frac{y_1(t)}{e_2(t)}; \dots; y_n(t) = \frac{y_{n-1}(t)}{e_n(t)}, (9)$$

The iteration stops at the nth step while $y_n(t) \leq 1$. It is obvious that $y_n(t)$ remains all the frequency information of $y(t)$, and the Hilbert transform is then applied to $y_n(t)$ to calculate the instantaneous frequency. The superiorities of NHT with respect to Hilbert transform in calculating the instantaneous frequency had been proved by Huang et al. (2009).

3. Time-frequency Analysis of Nonstationary Wind Speeds

3.1 *Nonstationary Wind Speed Data*

Typhoon Rammasun made landfall on the coastal region of Wenchang, Hainan Province on July 18th, 2014. The three-channel ultrasonic anemometer installed on a observation tower recorded the wind speeds during 16:00, July 17th and 13:00, July 19th (Beijing time) with a sampling frequency of 4Hz. The measured wind speeds are decomposed into the longitudinal, lateral and vertical wind speeds ($U(t)$, $V(t)$ and $W(t)$), and the time-history of the longitudinal wind speed is shown in Fig.1. The wind speed show clearly nonstationary features. The highest wind speed occurred around the 30th hour and was higher than 40 m/s. In this study, the wind speeds in the 30th and 32th (donated as H30 and H32, respectively) hours are taken as examples to study the nonstationary characteristics of the wind speeds. The longitudinal, lateral and vertical wind speeds at H30 and H32 are shown in Fig. 2.

The reverse arrangement test described by Bendat and Piersol (2010) is used to evaluate the stationarities of the wind speeds, and the results are listed in Table 1, in which N means nonstationary and S means stationary. Both $U(t)$ and $V(t)$ at H30 and H32 failed to pass the stationarity test, while both $W(t)$ pass the stationarity test.
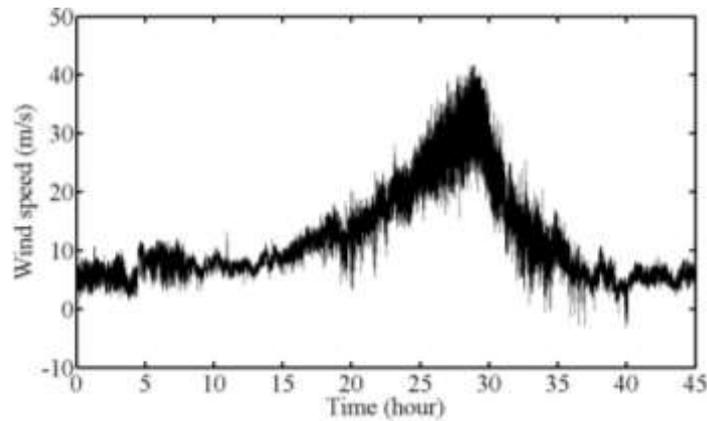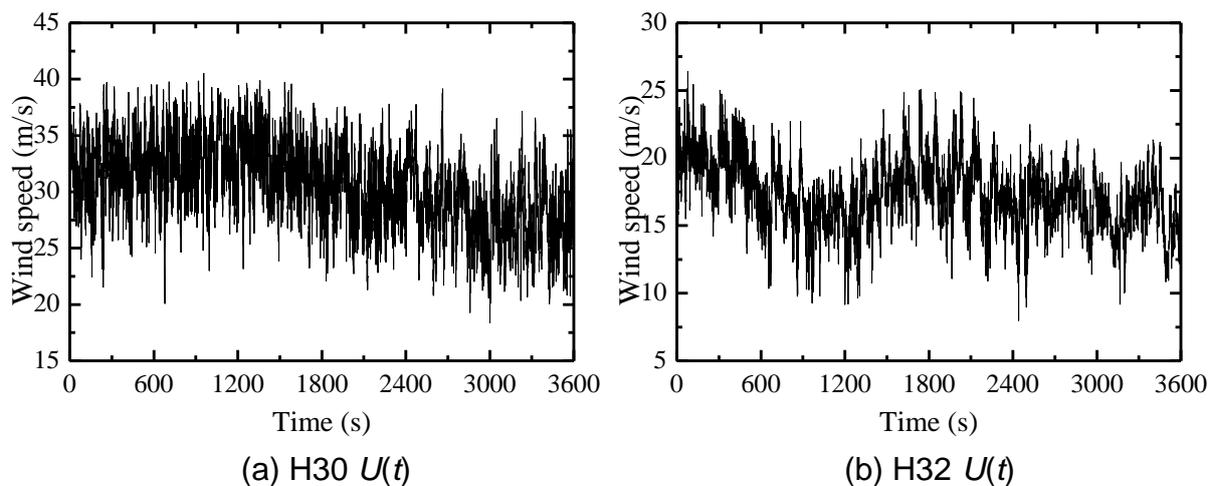

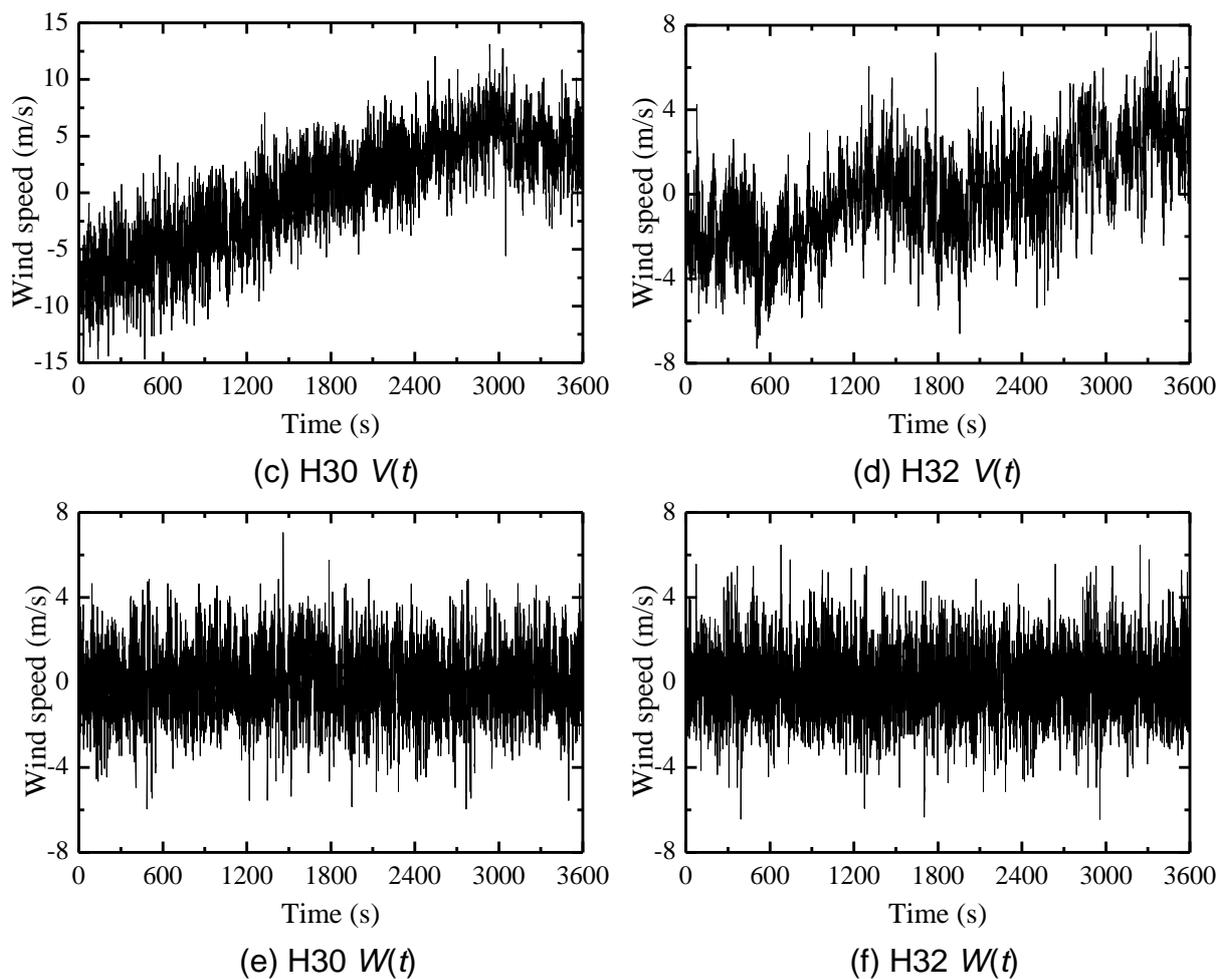Fig.1 Time-history of the longitudinal wind speed

(a) H30 $U(t)$ (b) H32 $U(t)$

(c) H30 $V(t)$

(d) H32 $V(t)$

(e) H30 $W(t)$

(f) H32 $W(t)$

Fig.2 Time-histories of nonstationary wind speeds

Table. 1 Stationary test results

Wind speed	$U(t)$	$V(t)$	$W(t)$
1	N	N	S
2	N	N	S

3.2 *Nonstationary Wind Speed Model*

The nonstationary features of extreme wind speeds have been noticed by researchers and they have modeled the longitudinal wind speed $U(t)$ as the summation of a time-varying mean and a zero-mean fluctuating component (Xu and Chen 2004)

$$U(t) = \bar{U}(t) + u(t), \quad (10)$$

where $\bar{U}(t)$ is the time-varying mean reflecting the temporal trend of wind speed; $u(t)$ is the fluctuating component.

However, the wind speeds data in the previous section show that the lateral wind speeds $V(t)$ also show clearly nonstationary features. Therefore, the nonstationary wind speed model is extended to

$$U(t) = \bar{U}(t) + u(t), (11a)$$

$$V(t) = \bar{V}(t) + v(t), (11b)$$

where $\bar{U}(t)$ and $\bar{V}(t)$ are the time-varying means in the longitudinal and lateral directions, respectively; $u(t)$ and $v(t)$ are the fluctuating components in the longitudinal and lateral directions, respectively. Generally, the highest frequency embedded in $\bar{U}(t)$ and $\bar{V}(t)$ should be sufficiently low (e.g. 1/5 ~ 1/10 of the fundamental vibration frequency of the concerned structure), so that their dynamic effects on structures can be neglected.

3.3 *Extraction of Time-varying Mean*

In this section, SWT and EEMD are used to extract the longitudinal and lateral time-varying means of the nonstationary wind speeds in Fig. 2. As mentioned above, the highest frequencies embedded in $\bar{U}(t)$ and $\bar{V}(t)$ should be sufficiently lower than the structural fundamental frequency. For most structures in civil engineering, their fundamental frequencies are higher than 1/32 Hz, e.g. the fundamental frequencies of the Guangzhou Tower (the 2nd highest building in the world) and the Akashi Kaikyo bridge (the longest bridge in the world) are 0.094Hz (Lei et al. 2012) and 0.039Hz (Minh et al. 2000), respectively. Therefore, 1/256 Hz ($1/8 \times 1/32$) is selected to be the highest frequency embedded in $\bar{U}(t)$ and $\bar{V}(t)$ in this study.

$U(t)$ for H32 is taken as an example to illustrate the process of extraction the time-varying mean. As mentioned above, the SWT behaves as a dyadic filter bank, the highest frequency of the approximation component is $f_s/2^{m+1}$. To make the highest frequency of the approximation component lower than 1/256, a 9 level decomposition was carried out by the db15 wavelet, and the results are shown in Fig. 3, in which level 1-9 indicate the details and level 10 indicates the approximation. Level 10 can then be treated as $\bar{U}(t)$. The weighted mean f_{mi} ($i = 1$ *to* 10) of the instantaneous frequencies of each level is listed in Table 2, which are calculated by

$$f_{mi} = \frac{\int f_i(t) a_i^2(t) dt}{\int |u_i(t)|^2 dt}, (12)$$

where $u_i(t)$ is the time-history of level i; $a_i(t)$ and $f_i(t)$ are the instantaneous amplitude and frequency of $u_i(t)$, respectively. $a_i(t)$ and $f_i(t)$ can be calculated by the NHT using Eq.

(6) and Eq. (7), and the results of level 8 are shown in Fig. 4. It can be seen that instantaneous frequency has high variance occasionally, which can be ascribed to the noises in the measured signal and the numerical error caused by the differentiation operation in Eq. (7). The instantaneous amplitude agrees well with the sampled peaks. Instantaneous frequencies and amplitudes of other levels are not shown here for brevity. The f_{mi} of level 10 is 0.003 Hz < 1/256 Hz, which further demonstrate that highest frequency of the approximation component is lower than 1/256 Hz.

The decomposition results of EEMD are shown in Fig. 5. It is found that 13 IMFs and a residue are generated by EEMD. The f_{mi} (i = 1 to 10) of each IMF is listed in Table 3. The f_{mi} of IMF 10 is 0.003 Hz < 1/256 Hz. Therefore, the summation of the 10th to 13th IMFs and the residue is treated as $\bar{U}(t)$.

The comparisons of the time-varying means extracted by SWT and EEMD are shown in Fig. 6. It can be seen that the time-varying means of these two methods are quite consistent and both reflect the trends of the nonstationary wind speeds satisfactorily.
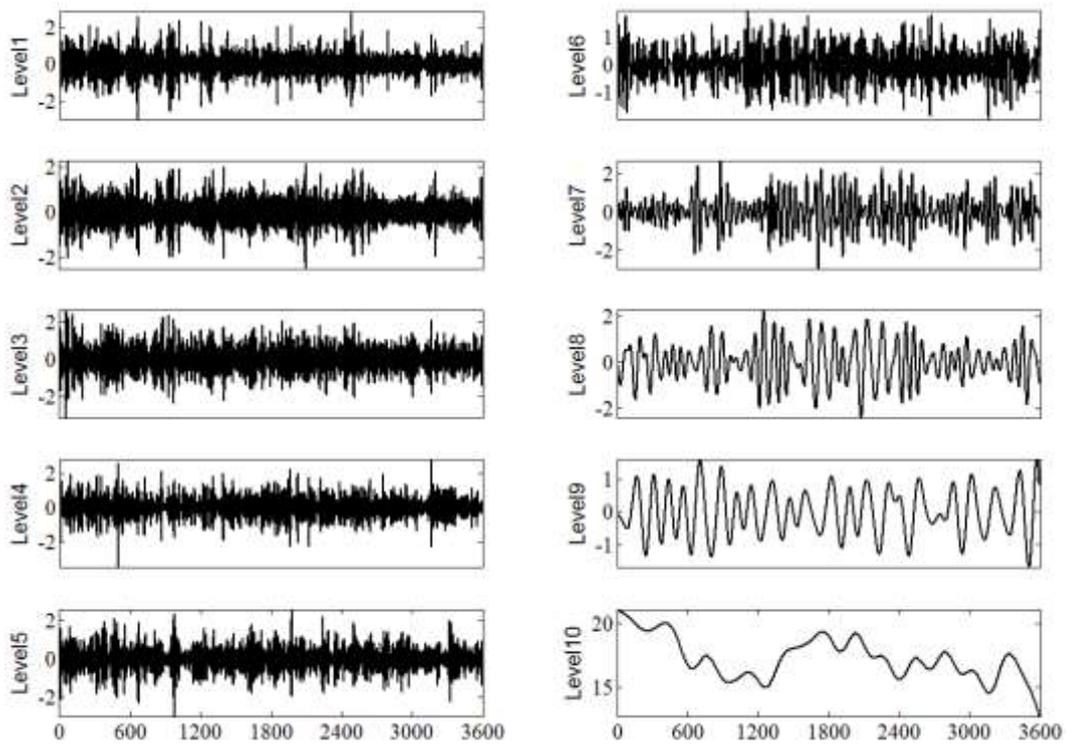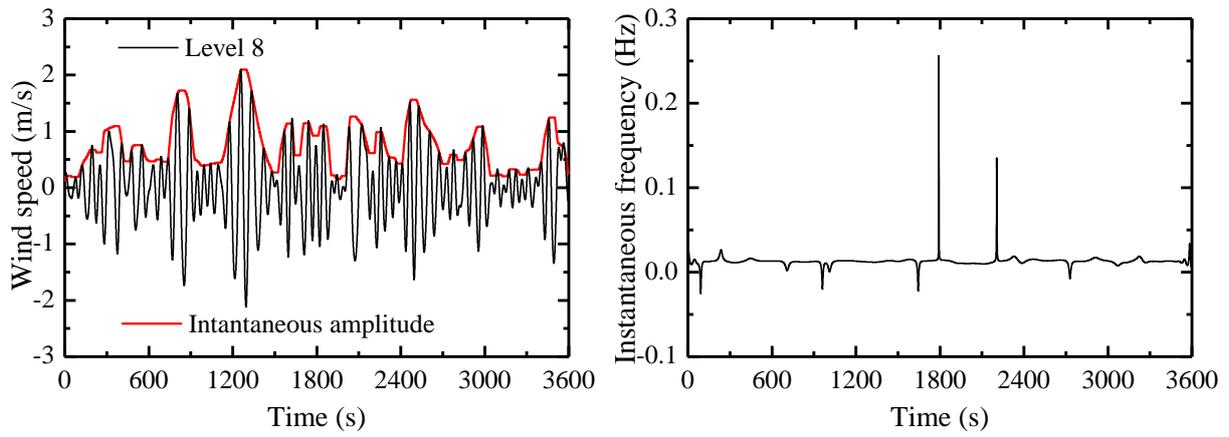

Fig. 3 SWT decomposition results for $U(t)$ at H32

Table. 2 f_m for different levels

Level	1	2	3	4	5	6	7	8	9	10
f_m	1.239	0.710	0.360	0.179	0.099	0.047	0.030	0.015	0.006	0.003

(a) Instantaneous frequency (b) Instantaneous amplitude
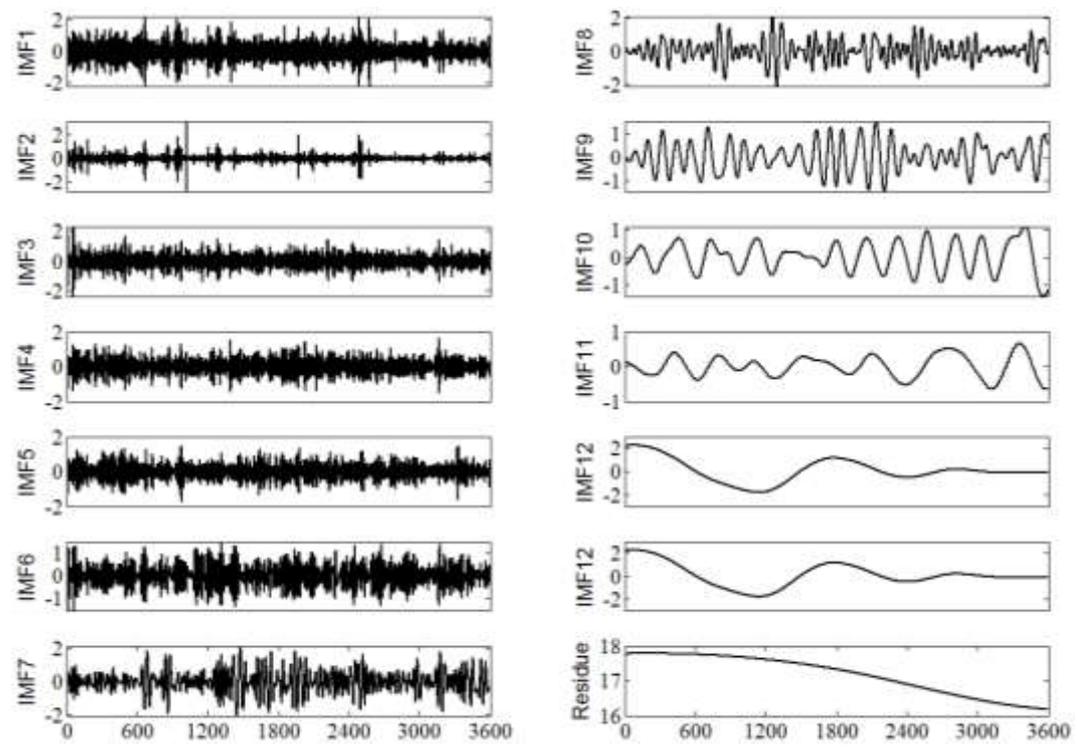Fig. 4 Instantaneous characteristics of level 8

Fig. 5 EEMD decomposition results for $U(t)$ at H32

Table. 3 f_m for different IMFs

IMF	1	2	3	4	5	6	7	8	9	10
f_m	1.237	0.765	0.374	0.214	0.109	0.051	0.030	0.015	0.006	0.003

(a) H30 $U(t)$ (b) H32 $U(t)$
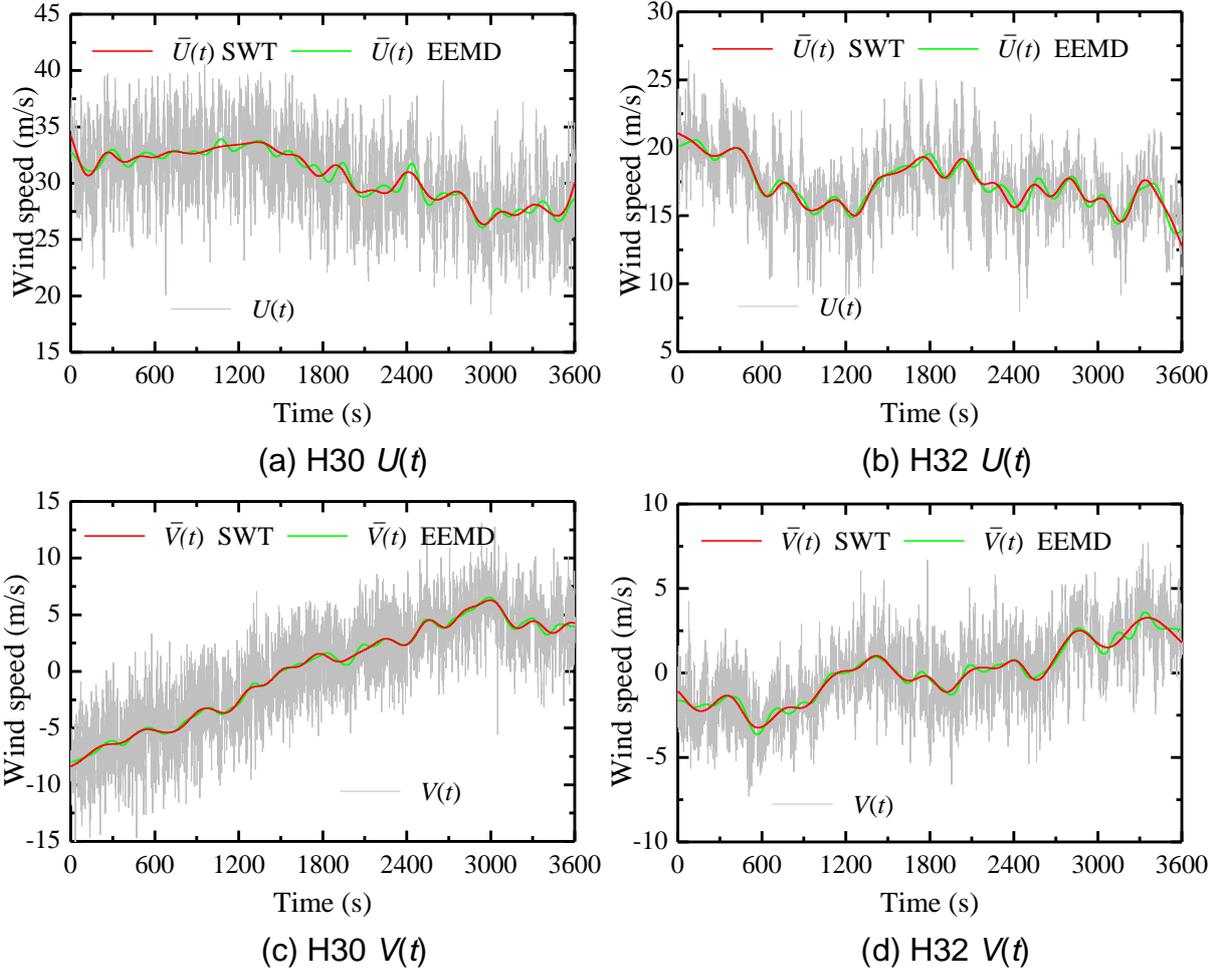
(c) H30 $V(t)$ (d) H32 $V(t)$

Fig.6 Time-varying means extracted by SWT and EEMD

3.3 *Time-frequency Analysis of the Fluctuating Components*

After extraction of the time-varying mean components, the fluctuating components can be expressed as the summation of 9 band-limited components, i. e.,

$$u(t) = \sum_{i=1}^{m} u_i(t), \text{(13a)}$$

$$v(t) = \sum_{i=1}^{m} v_i(t), \text{(13b)}$$

In this section, the Hilbert energy spectrum is used to characterize the time-frequency distribution of the fluctuation components. The Hilbert energy spectrum of the ith band-limit component is defined as
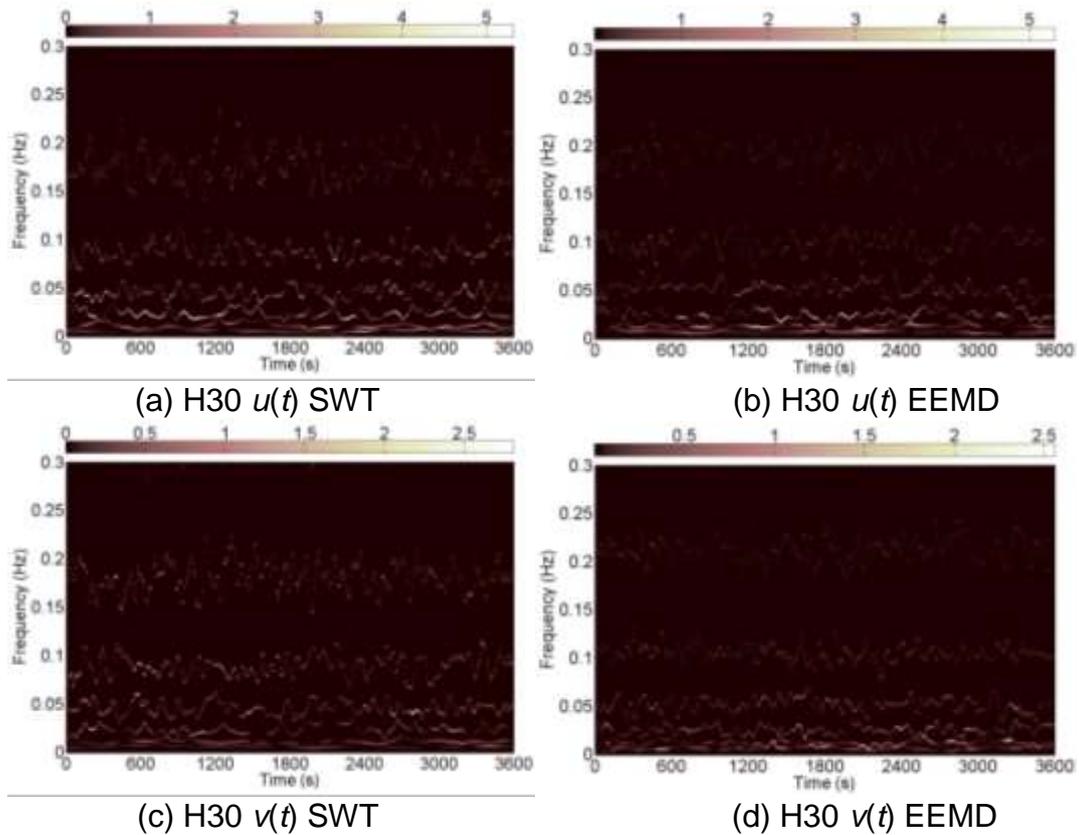
$$S_i(t,f) = \begin{cases} a_i^2(t), & f = f_i(t) \\ 0, & f \neq f_i(t) \end{cases}, \text{(14)}$$

Then, the time-frequency distributions of the fluctuation components can be described as

$$S(t,f) = \sum_{i=1}^{n} S_i[t,f(t)], (15)$$

As mentioned above, direct computation of instantaneous frequency using Eq. (7) may yield results with high variances as it is numerically sensitive and the signal is always contaminated by noises. A lot of measures have been taken to solve the problem (Huang et al. 1998, 2009; Spanos et al. 2007; Huang et al. 2015). In this study, a medium filter with the time interval $(t - 5, t + 5)$ s was used to reduce the variance, following Huang et al. (2015). Although the filtering degrades the time resolution, it makes the spectra readily amenable to physical interpretation.

The Hilbert energy spectra of the fluctuating components extracted by SWT and EEMD are shown in Fig 7. The intensities of the energies are illustrated by different colors. The frequency contents those higher than 0.3 Hz are not shown for their low energies and high variance of instantaneous frequencies. It can be seen that the spectra of the fluctuating components extracted by SWT and EEMD are quite consistent. The energy of the fluctuating components is mostly distributed in the frequency band lower than 0.1 Hz. The frequency modulations are weak, indicating that $u(t)$ can be modeled as an uniformly modulated nonstationary process (Chen and Letchford 2004; Huang et al. 2015).
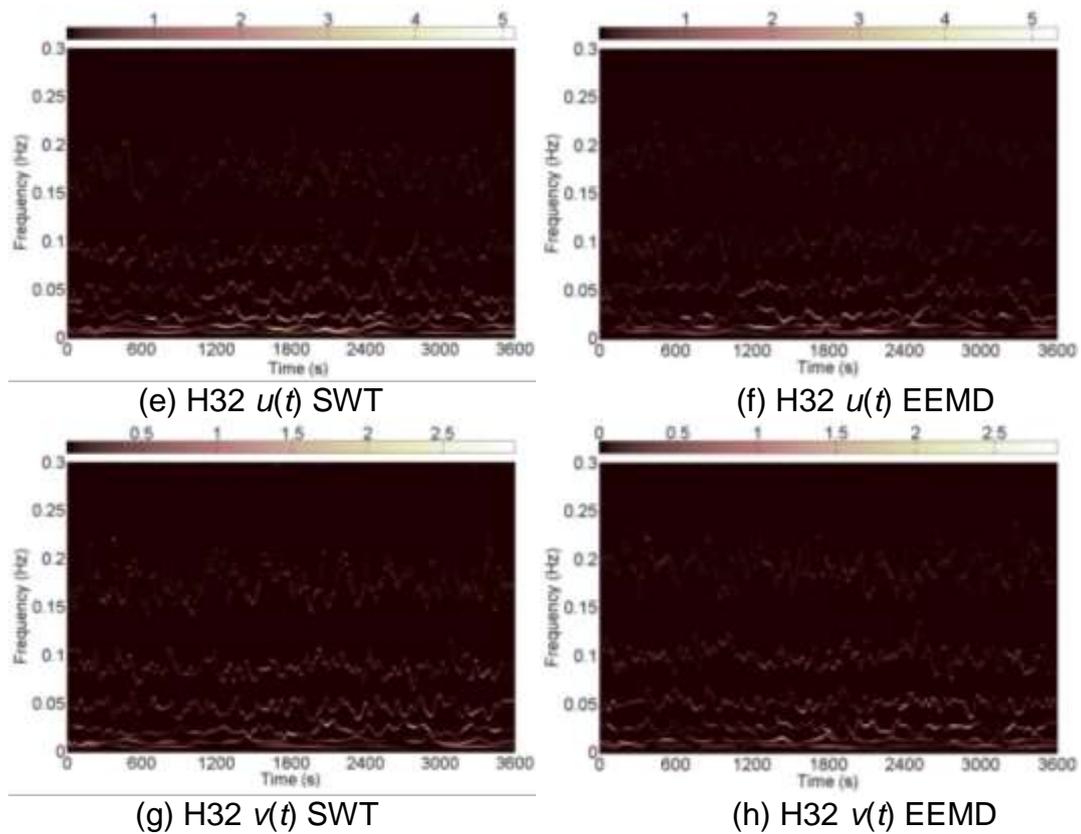

(a) H30 $u(t)$ SWT

(b) H30 $u(t)$ EEMD

(c) H30 $v(t)$ SWT

(d) H30 $v(t)$ EEMD

(e) H32 $u(t)$ SWT   (f) H32 $u(t)$ EEMD

(g) H32 $v(t)$ SWT   (h) H32 $v(t)$ EEMD

Fig 7 Hilbert energy spectra of fluctuating components

4. Conclusion

The paper analyzed the extreme wind speeds induced by typhoon Rammasun. The nonstationary wind speeds are decomposed into time-varying means and fluctuating components. The time-frequency distributions of the fluctuating components are characterized by the Hilbert energy spectra. Some main conclusions are summarized as follows:

1) Both the longitudinal and lateral wind speeds during typhoon show clearly nonstationary features.

2) Both the stationary wavelet transform and empirical mode decomposition are used to extract the time-varying means of the nonstationary wind speeds, and the results by the two methods are quite consistent.

3) The energies of the fluctuating components are mostly distributed in the frequency band lower than 0.1 Hz.

4) The frequency modulations of the fluctuating components are weak, indicating that the fluctuating components can be modeled as uniformly modulated nonstationary processes.

REFERENCES

Bendat, J. S., and Piersol, A. G. (2011). *Random data: analysis and measurement procedures.* Wiley, New York.

Carmona, R., Hwang, W. L., and Torrésani, B. (1998). *Practical Time-Frequency Analysis: Gabor and Wavelet Transforms, with an Implementation in S*. Academic Press, New York.

Chen, L., and Letchford, C. W. (2004). "A deterministic–stochastic hybrid model of downbursts and its impact on a cantilevered structure." *Eng. Struct.*, 26(5), 619-629.

Daubechies, I. (2004). *Ten lectures on wavelets*, Philadelphia: Society for industrial and applied mathematics.

Davenport, A. G. (1961). "The application of statistical concepts to the wind loading of structures." *Proc.Inst. Civ. Eng.*, 19(4), 449–472.

Davenport, A. G. (1967). "Gust loading factors." *J. Struct. Div.*, 93(3),11–34

Huang, G. Q., Su, Y. W., Kareem, A., and Liao, H. L. (2015). "Time-frequency analysis of nonstationary process based on multivariate empirical mode decomposition." *J. Eng. Mech.*, 142(1), 04015065.

Huang, N. E., Shen, Z., Long, S. R., W, M., Shih, H. H., Zheng, Q., Yen, N., Tung, C. C., and Liu, H. H. (1998). "The empirical mode decomposition and the Hilbert spectrum for nonlinear and non-stationary time series analysis." *Proc. R. Soc. Lond.*, 454, 903-995.

Huang, N. E., Wu, Z. H., Long, S. R., Arnold, K. C., Chen X. Y., and Blank, K. (2009). "On instantaneous frequency." *Adv. Adapt. Data Anal.*, 1(2), 177-229.

Holschneider, M., Kronland-Martinet, R., Morlet, J., and Tchamitchian, P. (1989) *A real-time algorithm for signal analysis with the help of the wavelet transform*. Springer, Berlin.

Kareem, A., Kijewski, T. (2002). "Time-frequency analysis of wind effects on structures." *J. Wind Eng. Ind. Aerodyn.*, 90(12), 1435-1452.

Lei, Y., Wang, H. F., and Shen, W.A. (2012). "Update the finite element model of Canton Tower based on direct matrix updating with incomplete modal data." *Smart Struct. Syst.*, 10(4-5), 471-483.

Li, Q. S., and Wu, J. R. (2007). "Time-frequency analysis of typhoon effects on a 79-storey tall building." *J. Wind. Eng. Ind. Aerodyn.*, 95(12),1648 –1666.

Mallat, S. G. (1989). "A theory for multiresolution signal decomposition: the wavelet representation." *IEEE T. Pattern Anal.*, 11(7), 674-693.

Minh, N. N., Yamada, H., Miyata, T., and Katsuchi, H. (2000). "Aeroelastic complex mode analysis for coupled gust response of the Akashi Kaikyo bridge model." *J. Wind Eng. Ind. Aerodyn.*, 88(2), 307-324.

Olhede, S., Walden, A. T. (2004) "The Hilbert spectrum via wavelet projections." *Proc. Roy. Soc. London, Ser. A.*, 460(2044), 955-975.

Percival, D. B., and Walden, A. T. (2000). *Wavelet Methods for Time Series Analysis*. Cambridge University Press, Cambridge, UK.

Spanos, P. D., Giaralis, A., and Politis, N. P. (2007). "Time-frequency representation of earthquake accelerograms and inelastic structural response records using the adaptive chirplet decomposition and empirical mode decomposition." *Soil Dyn. Earthquake Eng.*, 27(7), 675 –689.

Wang, L., McCullough, M., Kareem, A. (2013a) "A data-driven approach for simulation of full-scale downburst wind speeds." *J. Wind Eng. Ind. Aerodyn.*, 2013, 123: 171-190.

Wang, L., McCullough, M., Kareem, A. (2013b) "Modeling and simulation of nonstationary processes utilizing wavelet and Hilbert transforms." *J. Eng. Mech.*, 2013, 140(2), 345-360.

Wu, Z., Huang, N.E., (2009). "Ensemble empirical mode decomposition: a noiseassisted data analysis method". *Adv. Adap. Data Anal.*, 1(1), 1–41.

Xu, Y. L., and Chen, J. (2004). "Characterizing nonstationary wind speed using empirical mode decomposition." *J. Struct. Eng.*, 6(912), 912 –920.

Zhang, R. R., Ma, S., Safak, E., and Hartzell, S. (2003). "Hilbert-Huang transform analysis of dynamic and earthquake motion recordings." *J. Eng. Mech.*, 129, 8(861), 861–875.